SCIENTIFIC REPORTS

OPEN

SUBJECT AREAS:
FLUID DYNAMICS
FLUIDS
ELECTRICAL AND ELECTRONIC ENGINEERING
MECHANICAL ENGINEERING

Received
8 August 2014

Accepted
3 November 2014

Published
19 November 2014

Correspondence and requests for materials should be addressed to J.L. (jliubme@tsinghua.edu.cn)

Synthetically chemical-electrical mechanism for controlling large scale reversible deformation of liquid metal objects

Jie Zhang[1], Lei Sheng[1] & Jing Liu[1,2]

[1]Department of Biomedical Engineering, School of Medicine, Tsinghua University, Beijing, China, [2]Beijing Key Lab of CryoBiomedical Engineering and Key Lab of Cryogenics, Technical Institute of Physics and Chemistry, Chinese Academy of Sciences, Beijing, China.

Reversible deformation of a machine holds enormous promise across many scientific areas ranging from mechanical engineering to applied physics. So far, such capabilities are still hard to achieve through conventional rigid materials or depending mainly on elastomeric materials, which however own rather limited performances and require complicated manipulations. Here, we show a basic strategy which is fundamentally different from the existing ones to realize large scale reversible deformation through controlling the working materials via the synthetically chemical-electrical mechanism (SCHEME). Such activity incorporates an object of liquid metal gallium whose surface area could spread up to five times of its original size and vice versa under low energy consumption. Particularly, the alterable surface tension based on combination of chemical dissolution and electrochemical oxidation is ascribed to the reversible shape transformation, which works much more flexible than many former deformation principles through converting electrical energy into mechanical movement. A series of very unusual phenomena regarding the reversible configurational shifts are disclosed with dominant factors clarified. This study opens a generalized way to combine the liquid metal serving as shape-variable element with the SCHEME to compose functional soft machines, which implies huge potential for developing future smart robots to fulfill various complicated tasks.

Conventionally, most of the modern machines are fabricated with rigid materials, which however may encounter many restricted applications in certain specific requirements, such as owning capability of diverse flexible deformations, adaptability to unconventional environment, particularly passing through a narrow channel or uneven terrain. Based on the unique merit varying among different configurations and controllable locomotion, soft machines are competent for addressing many such tough issues which are hard to achieve otherwise through conventional rigid machines, especially when tackling some high-risk tasks. In order to obtain a desired reversible deformation or locomotion, tremendous efforts have been concentrated on developing various driving strategies, including pneumatic actuation[1,2], electric field-induced locomotion[3,4], magnetic force[5], biomimetic propulsion[6], light-driven rotation[7], materials-based actuation[8], temperature or pH actuation[9], surface-tension-driven self-folding[10], to name just a few. Among these methods, electric field is a rather versatile tool as its magnitudes, phases and frequencies are often easy to regulate.

Meanwhile, various materials such as hydrogels[9,11], photo-crosslinked polymers[12], acrylonitrile butadiene styrene (ABS)[2] and liquids[13] to compose soft devices have also been extensively investigated. Recently, a mountain of energy has especially been invested into the multifunctional material liquid metal, so as to exploit its potentials in various newly emerging areas, such as liquid metal enabled pump[14], memristor[13], heavy metal ion sensing[15,16], antennas[17,18], and printable ECG electrode[19] etc. The room temperature liquid metals such as gallium, eutectic GaIn (75% gallium and 25% indium) and Galinstan (68.5% gallium, 21.5% indium, and 10% tin) are quite appealing since they own a group of remarkable merits including super-compliance in liquid phase, high surface tension[20], favorable electrical conductivity[20], extremely low vapor pressure and low toxicity[21]. With an unusually large variation on surface-area-to-volume ratio and surface tension, the liquid metal was recently found to display outstanding performance of shape deformation[22]. Due to its inherent scalability, such material could easily

transform among diverse morphological states under the exposure to the external electricity. These behaviors are rather unique and extremely hard to achieve otherwise through conventional rigid materials and thus opened many opportunities to make soft machine. However, an only pity in our former efforts lies in that, the realized deformations of the liquid metal machine are overall mono-directional, which means that the liquid metal can transform from an extremely large sheet of thin film into a small sphere, but not vice versa. So far, reversible deformation of liquid metal among different configurations, which is the key to make a soft machine, still remains a big mystery.

Over the past continuous trials, we got to envision that if additional control mechanisms could be incorporated on the liquid metal, reversible deformation of machine thus made should be possible. Among the many potential effects, it is conceivable that the chemical dissolution on the surface of the liquid metal object would help realize strong deformation reversibly, since such configurational transformation was governed mainly by the surface tension. The key reason lies in that chemical dissolution can easily recover the surface tension through removing the oxide skin on the surface of the liquid metal, which is produced during the electrochemical oxidation process, and inversely reduces the surface tension. Such synthetically chemical-electrical mechanism (SCHEME) approach is liable to achieve the reversible deformation of the liquid metal which thus enables it as a smart material to manufacture soft machines in the near future. In this study, to clarify the main control issue of SCHEME, an object made of liquid metal gallium is adopted as the working machine to reconfigure itself into an arbitrary shape and reversibly deform between sphere and non-sphere states. Through altering the voltage, electrode spacing, electrolyte solution type or volume of the gallium machine, different performances of the material shape deformation are revealed. Overall, such reversible configurational transformation is achieved via the combination of electrochemical oxidation and chemical dissolution processes of oxide gallium, which can easily tune the surface tension of the liquid metal ranging from 700 mN/m[20] to near zero, upon application of the external electric field and alkaline or acidic electrolyte solution. To clarify the critical factors dominating the shape transformation of the working object, a series of comparative experiments were implemented and theoretical interpretations on the phenomena and mechanisms were carried out.

Results

As shown in Fig. 1A, a square insulated vessel with a cross-section of 12 cm × 12 cm is adopted to accommodate the gallium droplet and electrolyte solution. Two inert platinum electrodes with a diameter of 0.5 mm are employed, one of which is inserted into the metal droplet, while the other is placed in the surrounding electrolyte solution. To investigate the effect of the voltage between the two electrodes on the deformation, the applied voltage varies from 0 V to 30 V. In addition, different electrode spacings are prescribed since the distance between the two electrodes directly affects the intensity of the electrical field. On account that under the same electricity, the performance of the deformation is also related to the dosage of the liquid gallium, different volumes of gallium droplet are tested. In order to clarify the chemical events and thus evaluate the influence of electrolytes on the deformability and reversibility, the electrolytes including sodium hydroxide (NaOH), sodium sulfate (Na_2SO_4), sodium chloride (NaCl) and hydrogen chloride (HCl) solutions are adopted and comparatively investigated. The presented results are mainly obtained with NaOH solution, as the phenomena of the system operated with HCl solution are similar to those with NaOH solution. However, the deformation is significantly restricted when operating with Na_2SO_4 or NaCl solution, and the reversibility does not occur.

Generally, the liquid gallium forms into a spheroid in the aqueous solution through injection due to its high surface tension (~700 mN/m), and the hydrostatic pressure resulted from the gravity slightly distorts the shape, as seen in Fig. 1A. In the NaOH solution, gallium can react with the alkali solution slowly, producing gallates like $[Ga(OH)_4]^-$, which makes the surface of gallium negatively charged and cations accumulated nearby[14](Fig. 1A). Therefore, the electrically charged interface forms into a diffuse electrical double layer (EDL), which can be modeled as a charged capacitor. When an external power with the anode inserted into the gallium droplet and the cathode in the electrolyte solution is supplied, the previous equilibrium state will be broken up. Due to the high conductivity of the liquid metal gallium, the liquid metal droplet can be regarded as part of the anode. As a consequence, the ions on the surface of the droplet are altered, as shown in Fig. 1B. Conversely, anions accumulate near the droplet. As such, the EDL changes accordingly. The introduction of the external power supply reduces the initial surface tension of the liquid metal in a modest range when the applied power is not sufficient to produce electrochemical reaction. Under this circumstance, the relationship between the surface tension and the potential drop across the EDL has been thermodynamically analyzed, which is known as electrocapillary for an ideal model[19]. Such relationship can be described by the integrated Lippmann's equation[14,23,24], which has been verified through a large number of experiments with many different setups and various electrolytes[23], i.e.

$$\gamma = \gamma_0 - \frac{1}{2} c V^2 \tag{1}$$

where, γ is the surface tension, c is the capacitance of electric double layer per unit area, V is the potential difference across the EDL, γ_0 is the maximum surface tension when $V = 0$[23].

Following the Young-Laplace equation, the pressure difference p across the electrolyte and the liquid metal droplet can be given as follows[14]:

$$p = \gamma \cdot \frac{2}{r} \tag{2}$$

where, $1/r$ is the curvature of the droplet surface. From the Eq.(2), with slight decrease of the surface tension, the pressure difference p across the electrolyte reduces modestly. Thus, the deformation of the liquid metal droplet is not obvious, and the liquid metal behaves in a manner similar to the classic electrocapillary effect.

Realization of large-scale reversible deformation. With the application of the external electrical potential above a critical value, redox reaction between the two electrodes proceeds. Since platinum is inert metal and the electrolyte is NaOH, the reduction reaction on the cathode produces hydrogen, while the oxidation reaction on the anode is divided into two parts: oxygen is electrochemically formed on the platinum electrode, of which part contacts with the electrolyte solution, while a thin layer of gallium oxide is produced on the surface of the liquid metal gallium. The surface tension of the liquid metal drops substantially with the formation of the solid oxide layer (explained in SI Appendix, Section 1), which induces the droplet into a pronounced nonspherical shape[21], as seen in Fig. 1B and Fig. 1C. The mass of the products on the anode, including oxygen and the oxide gallium, can be calculated according to the Faraday's law of electrolysis as follows:

$$m = kIt \tag{3}$$

$$k = \frac{Mq}{Fn} \tag{4}$$

where, m is the mass of the products on the anode, I and t are the intensity of the electric current and power-on time, respectively, k is the electrochemical equivalent, M is the molar mass of the products on the anode, n is the valency of the products, and F=9.65*104 C/mol is the Faraday's constant. Though the products on the anode

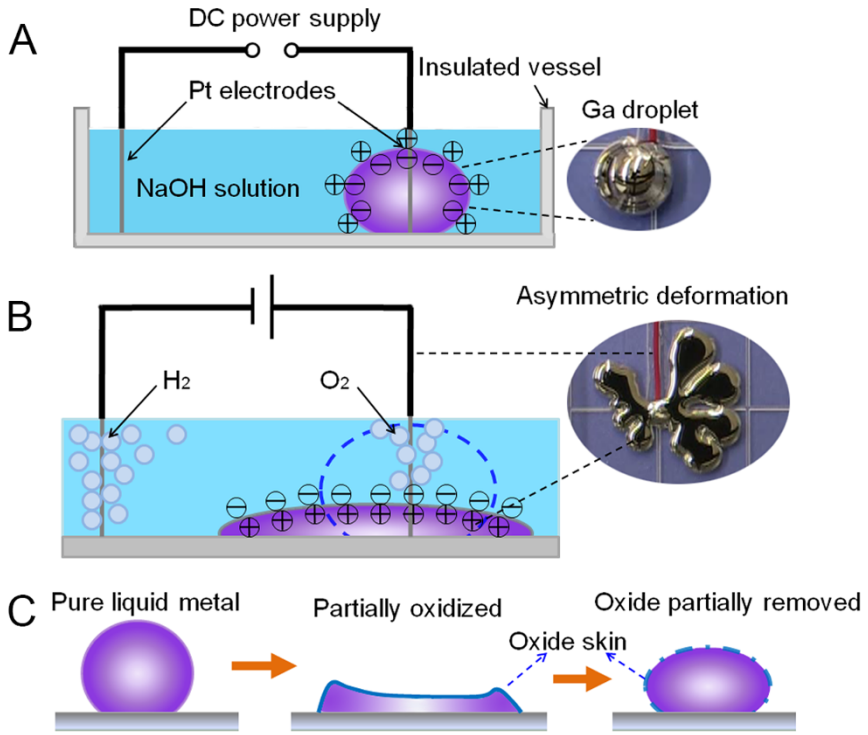

Figure 1 | Working mechanism of the reversible liquid metal deformation. (A) Schematic of the experimental setup without external power supply when the gallium droplet is placed in the NaOH solution. (B) Schematic of the gallium droplet surface charge redistribution when the direct power is applied. (C) The surface tension dominates deformation of liquid metal object along with the accumulation and dissolution of the oxide layer.

consist of oxygen and the oxide gallium, the amount of the oxide layer still depends on the intensity of the electric current and the power-on time. As the oxide gallium can react with NaOH solution, the oxide layer is dissolved in the solution at the same time of its formation, and the dissolution of the gallium oxide recovers the surface tension of the liquid metal, which renders the metal back into a spheroid, as shown in Fig. 1C. Additionally, the dissolution rate depends on the concentration and temperature of NaOH solution. In fact, with fixed electrode spacing and fixed concentration of NaOH solution under a constant temperature, the voltage affects the current intensity directly. Thus, the external voltage can be applied to adjust the electrochemical reaction and the consequent liquid metal deformation. In general, the gallium droplet spreads along with the production of the oxide layer. Since the solid oxide layer hinders the flow of the liquid metal, the dissolution also affects the deformability. Moreover, the reversible reconfiguration is governed by the dissolution of the oxide layer.

Interpretation of the major factors to dominant the reversible deformation. Obtained by Faraday's law of electrolysis (Eq.(3) and Eq.(4)), the formation rate of the oxide gallium F_{rate} can be calculated as follows:

$$F_{rate} = \frac{dm}{dt} = kI = \frac{Mq}{Fn} \cdot \frac{U}{R} \tag{5}$$

where, U is the external voltage and R is the electrical resistance along with the electric current path. Here, U/R is used to approximate the electric current for simplification. The deformability depends on the accumulation of the solid oxide gallium to some extent, which renders the surface tension to drop suddenly.

Obviously, the electrical resistance R is the function of both the electrode spacing and electrolyte concentration. The relationship is expressed with the introduction of the abstraction function f as follows:

$$R = f(c,d) \tag{6}$$

where, c and d denote the concentration of the electrolyte and the electrode spacing, respectively. Though the variables c and d are not exactly linear to the electrical resistance R, the change of R by c and d is clear: larger concentration reduces the electrical resistance, while larger electrode spacing increases it.

As aforementioned above, the deformability and reversibility rely on the dissolution of the oxide gallium. The dissolution rate D_{rate} is related to the acid-base property of the electrolyte solution, the concentration of the electrolyte solution, the contact area between the electrolyte solution and the oxide skin, and the temperature of the solution. Here, another abstraction function g is introduced to describe the relation between the dissolution rate and these variables:

$$D_{rate} = g(c,s,T) \tag{7}$$

where, c, s and T are concentration of the electrolyte solution, contact area and temperature of the solution, respectively. Eq.(7) is only applicable under the condition that the electrolyte is acidic or alkaline. Both higher concentration c and larger contact area s can accelerate the dissolution rate. Thereinto, contact area s depends on the gallium volume and the deformation, and thus it dynamically changes during the extension and contraction process. The temperature should be higher above the melting point of gallium to maintain fluidity of the liquid metal, and the dissolution rate increases along with the rise of the temperature.

It is noteworthy that the reversible deformation mainly depends on the formation rate of the oxide gallium F_{rate} and dissolution rate D_{rate}, but is not limited thereto. Theoretically, both the size and material of the working electrode affect the deformation, as the electrode size affects the initial contact area c slightly and the anode material has an impact on the oxidation reaction. Furthermore, the hydrogen produced on the cathode provides an opposite force to push the gallium away, which is quite obvious when the liquid

metal approaches to the cathode and the production of hydrogen is evident.

Effect of the applied voltage and electrode spacing on the liquid metal deformability. Fig. 2A, B and C illustrate the reversible deformation of liquid metal object in response to the voltage of 10 V, 20 V and 30 V, respectively (also shown in Supplementary Movie S1, Movie S2 and Movie S3). As the power-on time progresses, the metal extends gradually. As the drop of electric current across the EDL is less on the side toward the cathode, the formation of the oxide gallium becomes faster on this side, and thus the deformation near the cathode is prior to that far away from the cathode (detailed in Supplementary SI Appendix, Section 1). Consequently, the deformation turns out to be asymmetric and extends to the cathode in advance of the other location away from the cathode. Interestingly, when the surface spreads to a certain degree, the metal forms an irregular shape like petals (Fig. 2B). The speed of extension, which is faster in the first two seconds than that in the last three seconds (Fig. 2D), especially in the condition of 10 V and 30 V, depends heavily on the voltage. However, the main reasons of such speed difference in the last three seconds are not the same: upon the 10 V voltage, along with the deformation, the area contacting with the solution increases, which accelerates the dissolution process, and thus the formation of the oxide layer basically keeps up with the dissolution process; With the application of 30 V voltage, the formation of oxide gallium appears much faster than the dissolution all the time, which causes oxide layer to accumulate continuously. And in the first two seconds, the surface of the metal has not yet been totally coated with the oxide layer, which induces the deformation, while in the last three seconds, the totally coated oxide layer is only thickened, which hampers the further deformation (Fig. 2C). After five seconds, the direct voltage is removed, and the metal reconfigures itself into a sphere reversibly. With the increase of the voltage, more gallium oxide is accumulated, and thus the recovery rate decreases, as shown in Fig. 2D. The detailed effect of the voltage on the reversible deformation is explained in Supplementary SI Appendix, Section 2.

To further explore the representative characteristics of the reversible deformation, a series of comparative experiments are conducted. First of all, in the absence of NaOH electrolyte, i.e. in the deionized water, no deformation occurs, demonstrating that the deformation does not simply rely on the potential difference. Secondly, when adding NaOH electrolyte in the deionized water, obvious change of the droplet morphology is observed, confirming that it is the electric current that results in the deformation. With the application of the external direct power, the electric current depends on the voltage as well as the concentration of the electrolyte solution, as indicated in Fig. 3A. Whether increasing the voltage or raising the solution concentration can improve the electric current, and the electric current is not constant during the deformation since the deformation disturbs the current circuit. As for voltage, at the beginning, the performance of the deformation is enhanced along with the increase of the voltage, while it decreases when the voltage is above a critical value, as shown in Fig. 3B. This is mainly due to that the continuous accumulation of the solid oxide layer hampers the further deformation (Fig. 2C). Besides, in response to the same applied voltage, enlarging the distance between the two electrodes renders the electric current path with larger electrical resistance, and consequently the relative electric current is reduced, which weakens the electrochemical reaction, as expressed in Eq. (2). As a result, with the exposure to the same low voltage and larger distance, smaller deformability is obtained (Fig. 3B). However, as the voltage continuously increases, the deformation performance is improved with larger distance since the evident oxidation is relatively weaker than that with shorter distance, as shown in Fig. 3B.

Effect of the concentration and acid-base property of electrolyte on the deformation. Though under the same voltage and electrode spacing, raising the concentration of the NaOH solution can reduce the electrical resistance of the current path and thus increase the

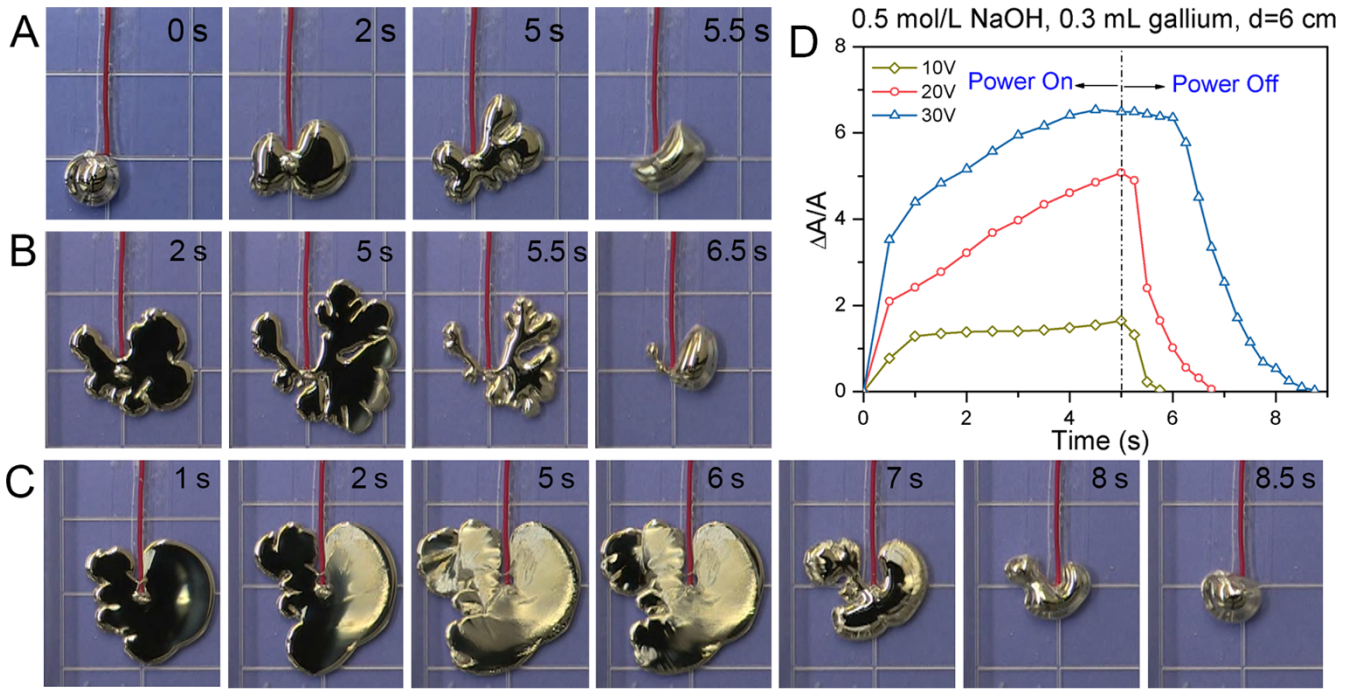

Figure 2 | The reversible deformation with 6 cm electrode spacing and 5 s power-on time under the condition of 0.3 mL liquid gallium and 0.5 mol/L NaOH solution at 32°C. (A), (B) and (C) are sequential snapshots when 10 V, 20 V and 30 V direct voltages are applied, respectively. (D) The relative change of the cross sectional area along with the time. The symbol ΔA and A respectively refer to the change of the cross sectional area and the original cross sectional area upon 0.3 mL liquid gallium.

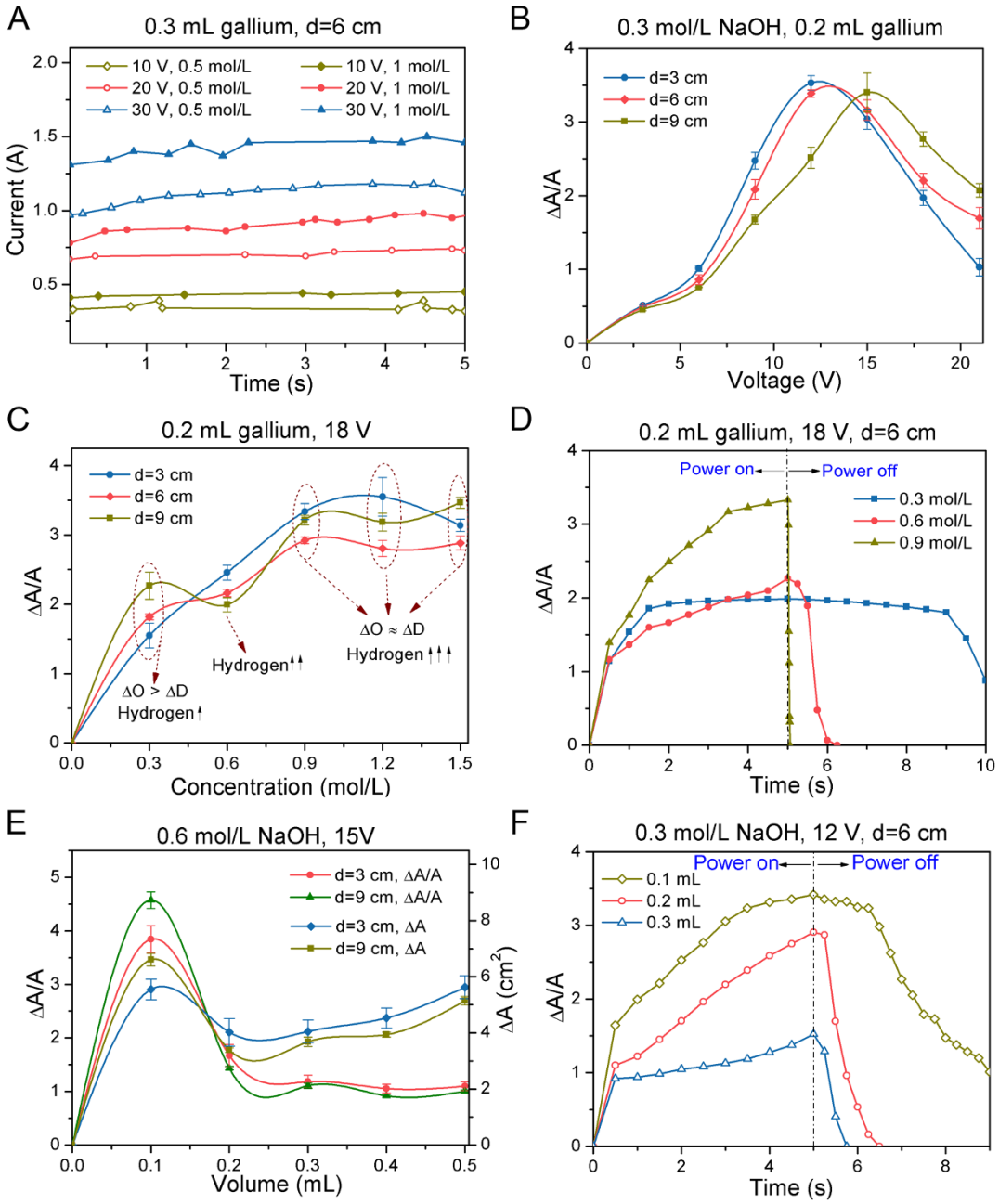

Figure 3 | The exploration of the main factors affecting the reversible deformation. The left vertical coordinate of (B) – (F) all refer to the relative change of cross sectional area, where the symbol ΔA and A denote the change of the cross sectional area and the original cross sectional area, respectively. The power-on time lasts for five seconds. (A) The electric current in response to different voltages. (B) The relative change of cross sectional area at the fifth second under different electrode spacings and voltages. (C) The relative change of cross sectional area at the fifth second with different concentrations of NaOH solution and electrode spacings. The symbols ΔO and ΔD denote the rate change of oxidation and dissolution, respectively. (D) The relative change of cross sectional area along with the time under different concentrations of NaOH solution. (E) The relative change of the cross sectional area (the left vertical axis) and change of cross sectional area (the right vertical axis) at the fifth second with different volumes of liquid gallium and electrode spacings. (F) The relative change of cross sectional area along with the time under different volumes of the liquid droplet.

electric current, as shown in Fig. 3A, the performance of the liquid metal deformation is not improved in the high concentration of NaOH solution as the concentration affects the dissolution of the oxide layer as well (Fig. 3C, Supplementary Movie S3 and Movie S4). At this stage, it is challenging to quantify the exact relation between the deformability and concentration of the NaOH solution since the increase of the concentration accelerates both oxidation and dissolution, as demonstrated in Eq.(5), (6) and (7), respectively (also explained in Supplementary SI Appendix, Section 3). As displayed in Fig. 3C, upon the exposure of 18 V voltage, the increment of the oxide accumulation becomes much larger than that of the oxide dissolution in 0.3 mol/L NaOH solution. As a result, the deformation is improved along with longer electrode spacing. In contrast to the 0.3 mol/L NaOH solution, the result is inverse in 0.6 mol/L NaOH solution since the oxidation does not obviously hinders the deformation. However, there is no significant difference when the experiment is operated in 0.9, 1.2 or 1.5 mol/L NaOH solutions, respectively (Fig. 3C) since the increments of both oxide accumulation and dissolution are approximately the same. In the high concentration solution, the opposite force acting on the

liquid metal from the production of the hydrogen cannot be neglected as such force impedes the deformation towards the cathode, especially when operating with shorter electrode spacings (Fig. 3C). Therefore, it is reasonable to explain the fluctuation phenomenon in the relatively high concentration case of NaOH solution (Fig. 3C). Assuming an ideal situation that when the voltage and electrode spacing are determined, a certain concentration of NaOH solution makes the oxidation speed approximate to that of the oxide dissolution, the deformation is minimized. It is noteworthy that in the high concentration of the NaOH solution, a shorter electrode spacing may cause the change of the metal morphology smaller since the deformation is so fast that the petals are ruptured and reversibly form into several spheres instantly, such as in the 1.5 mol/L NaOH solution with 3 cm electrode spacing as shown in Fig. 3C. The newly formed spheres either scatter or recombine with the rest petals and deform again until the direct power is switched off. As shown in Fig. 3D, upon the 18 V voltage and 0.3 mol/L NaOH solution, the deformability is extremely limited as the oxide layer is coated on the surface of the liquid metal very fast and hampers the deformation, which can be observed that from the 2 s to the 5 s the deformation is barely unchanged and when the power is turned off, it takes about 4 s when the morphology of the liquid gallium starts to recover. However, in the 0.9 mol/L NaOH solution, the deformation performance increases, and the speed of the extension becomes much faster. Meanwhile, the reversibility accelerates and takes less than 0.1 s to retract back into a sphere or several smaller spheres (Fig. 3D), which is mainly caused by that the high concentration induces less accumulation of oxidation and dissolves the oxide skin much faster. To demonstrate that it is the dissolution of the oxide layer that regulates the reversibility, a series of control experiments are conducted. Instead of NaOH electrolyte, Na_2SO_4 solution has also been studied with the reason that it cannot dissolve the oxide gallium. As a result, though the electrochemical reaction renders the neutral solution to alkalinity, the deformation is still rather limited, and the metal cannot reconfigure itself into a sphere. After the deformation of the gallium in the Na_2SO_4 solution, when adding appropriate NaOH or HCl solution on the liquid metal surface, the deformed droplet recovers back into a sphere slowly (shown in Supplementary Movie S5), confirming that the key mechanism of the reversibility is really based on the dissolution of the oxide layer. Clearly, the concentration of NaOH solution is the main factor to regulate the reversibility.

Effect of the liquid metal volume on the deformability. To investigate the operation of the reversible deformation under different amounts of the gallium, several typical volumes of the droplet from 0.1 mL to 0.5 mL have been studied. The relative change of the cross sectional area is not simply reduced with the increase of the metal, as shown in Fig. 3E. With 15 V voltage and in 0.6 mol/L NaOH solution, the relative change of the morphology is the largest upon 0.1 mL gallium, while it reduces when increasing the volume of gallium droplet (Fig. 3E). From 0.3 mL to 0.5 mL of liquid gallium, the relative change of the cross sectional area is not obvious, and the change of the total morphology slightly increases, though the production of the oxide gallium cannot cover the whole droplet and the larger original surface of the gallium is conducive to dissolve the thin oxide layer. It mainly results from that larger droplet is closer to the cathode at the initial time, and thus the formation of the oxide gallium is a little bit more than that with smaller droplet. In contrast to the experiment in 0.6 mol/L NaOH solution with 15 V voltage, the deformation in the 0.3 mol/L with 12 V voltage is quite different (Fig. 3F): the relative change of the cross sectional area declines upon with 0.1 mL gallium, while it rises upon 0.2 mL gallium since the aggravated oxide accumulation restricts the deformation of 0.1 mL liquid gallium and contributes to the extension of 0.2 mL gallium inversely; In response to 0.3 mL gallium, the relative change does not differ evidently since the larger initial surface of the liquid gallium accelerates the dissolution of the oxidation since the area contacting with the alkali solution is also larger. Moreover, the average thickness of the oxide layer becomes thinner as the oxide gallium should be distributed on the whole surface of the droplet, which results in that the oxidation is not sufficient to contend against the dissolution. According to the Faraday's Law in Eq. (3) and (4), under the same condition except for the amount of gallium, the output of the oxidation obtained from different volumes of gallium varies slightly if ignoring the effects of volume and the deformation on the electric current. Theoretically, though the output of the oxidation is almost the same, the original surface affects the dissolution. Therefore, compared with larger droplet, the retraction speed with smaller droplet is lower as the contacting area with the solution is less (Fig. 3F), which slows down the dissolution (explained in Supplementary SI Appendix, Section 4, Supplementary Movie S3 and Movie S6).

Deformation induced by low and periodic voltage. When a 10 Vp-p square-wave signal connecting with a 50 Ω in series is applied, the low voltage loading on the liquid metal makes its morphology regular and circularly symmetric (Supplementary Movie S7 and Movie S8). In addition, the change of the morphology is periodic along with the power supply. Fig. 4A and Fig. 4B respectively show the relative change of the cross sectional area with frequency of 1 Hz and 0.5 Hz. Under such low frequency and periodic voltage, the behavior of the droplet is similar to heartbeat, rhythmically relaxing and contracting. When the gallium extends to some degree, prolonging the power-on time will not increase the relative change since the oxidation reaches its equilibrium state with dissolution dynamically. In contrast to the square wave, the periodic voltage with sine wave can slow down the rate of extension and contraction.

Deformation induced by larger size of electrodes or unfixed cathode. Taking the size of the electrodes into account, graphite electrodes with 2 mm diameter are adopted. The oxygen generated on the anodal graphite electrode is much more than that on the anodal platinum electrode as the contacting area with the alkali solution on the anodal graphite electrode is much larger. Actually, the change of liquid metal morphology induced by the graphite electrodes cannot be neglected, especially when the dosage of the gallium is only a small amount. In addition, the size of the graphite electrodes affects the distribution of the electric field in the solution, and consequently affects the oxidation. Interestingly, when moving the cathodic graphite electrode, the liquid metal locomotes following the cathodic graphite electrode, as revealed in Fig. 4C and Fig. 4D. The deformation tends to spread toward the cathode, while the hydrogen produced on the cathode pushes the metal aside (Supplementary Movie S9).

Conclusion and Discussion

In summary, we have discovered for the first time the liquid metal-based reversible shape transformation phenomenon enabled by the SCHEME. The main mechanism for such large scale material deformation comes from the combined electrolytic oxidation and the dissolution effect, as demonstrated by a series of comparative experiments in the present work. Further, to disclose the major factors in dominating the deformation behavior, a series of typical conditions have been investigated and evaluated, including the concentration and acid-base property of the solutions, the external electrical voltage, the electrode spacing, the size of the electrode and the volume of the gallium objects etc. As it was revealed, all these factors affecting the deformability are closely related to the electro-

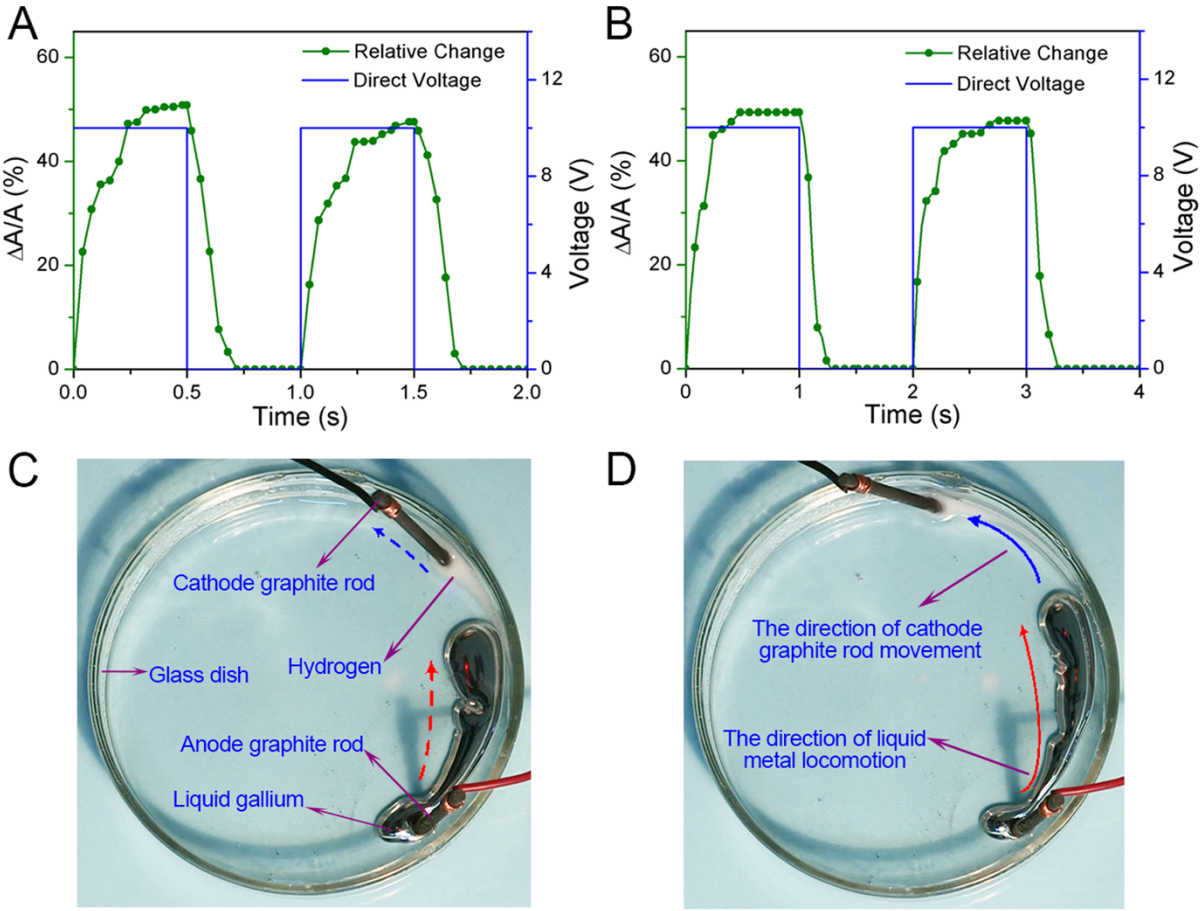

Figure 4 | The periodic deformation and the locomotion following the movement of the cathode. The concentration of the applied NaOH solution is 1.0 mol/L. The left vertical coordinate of (A) and (B) both refer to the relative change of cross sectional area, where the symbol ΔA and A denote the change of the cross sectional area and the original cross sectional area, respectively, while the left coordinate refers to the applied voltage. In (A) and (B), the electrode spacing and the volume of the gallium are respectively 3 cm and 0.2 mL. (A) The frequency of the square wave voltage is 1 Hz. (B) The frequency of the square wave voltage is 0.5 Hz. In (C) and (D), the volume of the gallium is 0.4 mL, and the electrodes are graphite rods with diameter of 2 mm.

chemical reaction and chemical dissolution mechanisms. It is important to notice that the material extension rate is under control of the electrical voltage and the concentration of the acidic or alkaline solution, while the retraction rate immensely depends on previous oxide accumulation and concentration of the acidic or alkaline solution. Since the reversibility relies heavily on the chemical dissolution, the primary task for controlling such reversible deformation is to identify the appropriate electrolyte solution and its optimum concentration. As a result, the applied voltage and the electrode spacing can be designated to realize the expected deformation. Further, experiments on the periodic voltage and locomotion of the metal with the unfixed cathode also revealed more interesting phenomena. Overall, it can be seen that the present principle has generalized adaptability. For example, the liquid metal material with strong shape changeable capabilities is not only restricted to the gallium as intensively tested here. More candidate materials can in fact be easily found among quite a few room temperature liquid metals. For example, if simply adopting the metal fluids such as eutectic gallium-indium alloy $GaIn_{25}$ (75% gallium and 25% indium) or Galinstan (68.5% gallium, 21.5% indium, and 10% tin) as the testing machine, similar phenomena can be observed. Further, such shape transformational behavior can also naturally be extended to various pre-designed device structures or patterns to realize desired tasks according to specific needs. But to focus on the core issue, these redundant results or data will not be provided here for brief. In general, the SCHEME as proposed here opens a basic strategy of utilizing liquid metal as smart material to manufacture soft machines. Meanwhile, the disclosed reversible deformation phenomenon also offers an exciting platform for developing diverse applications that cannot easily be achieved through rigid materials, such as functioning as flexible components, assembling electronic devices, and eventually realizing a dynamically programmable and reconfigurable soft robot in the near future.

Methods

Before the experiments, both the gallium and the electrolyte solutions were placed separately in different beakers, and the temperatures of these beakers were maintained at 45°C in an electro thermostatic water bath. The experiments started with the addition of 80 mL electrolyte solutions and the injection of a drop of liquid metal gallium into an insulated vessel. The voltage between the inert platinum electrodes was generated by a direct power supply (Long Wei, PS-305D, Hong Kong, China). The transient images of the dynamic deformation of the testing objects were captured by a high-speed camera (Canon XF-305, Japan). To obtain the periodic voltage, a digital signal generator (RIGOL, DG 1032Z 30-MHz Dual Channel, China) was employed. All the experiments were repeated by 8 times and the data was presented as mean ± standard deviation.

1. Mosadegh, B. *et al.* Control of soft machines using actuators operated by a Braille display. *Lab Chip.* **14**, 189–199 (2014).
2. Shepherd, R. F. *et al.* Multigait soft robot. *Proc Natl Acad Sci USA.* **108**, 20400–20403 (2011).
3. Tang, S. Y. *et al.* Electrochemically induced actuation of liquid metal marbles. *Nanoscale.* **5**, 5949–5957 (2013).

4. Loget, G. & Kuhn, A. Electric field-induced chemical locomotion of conducting objects. *Nat Commun.* **2**, 535-1-6 (2011).
5. Zhang, K. *et al.* On-chip manipulation of continuous picoliter-volume superparamagnetic droplets using a magnetic force. *Lab Chip.* **9**, 2992–2999 (2009).
6. Nawroth, J. C. *et al.* A tissue-engineered jellyfish with biomimetic propulsion. *Nat Biotechnol.* **30**, 792–797 (2012).
7. Eelkema, R. *et al.* Nanomotor rotates microscale objects. *Nature.* **440**, 163–163 (2006).
8. Cameron, C. G. & Freund, M. S. Electrolytic actuators: alternative, high-performance, material-based devices. *Proc Natl Acad Sci USA.* **99**, 7827–7831 (2002).
9. Yoon, C. K. *et al.* Functional stimuli responsive hydrogel devices by self-folding. *Smart Mater Struct.* **23**, 094008 (10pp) (2014).
10. Kaplan,R., Klobušický, J., Pandey, S., Gracias, D. H. & Menon, G. Building polyhedra by self-assembly: theory and experiment. *Artif Life.* **20**, 409–439 (2014).
11. Calvert, P. Hydrogels for soft machines. *Adv Mater.* **21**, 743–756 (2009).
12. Jamal, M., Zarafshar, A. M. & Gracias, D. H. Differentially photo-crosslinked polymers enable self-assembling microfluidics. *Nat Commun.* **2**, 527 (6pp) (2011).
13. Koo, H. J., So, J. H., Dickey, M. D. & Velev, O. D. Towards all-soft matter circuits: Prototypes of quasi-liquid devices with memristor characteristics. *Adv Mater.* **23**, 3559–3564 (2011).
14. Tang, S. Y. *et al.* Liquid metal enabled pump. *Proc Natl Acad Sci USA.* **111**, 3304–3309 (2014).
15. Sivan, V. *et al.* Liquid metal marbles. *Adv Funct Mater.* **23**, 144–152 (2013).
16. Tang, S. Y. *et al.* Liquid metal actuator for inducing chaotic advection. *Adv Funct Mater.* DOI: 10.1002/adfm.201400689 (2014).
17. So, J. H. *et al.* Reversibly deformable and mechanically tunable fluidic antennas. *Adv Funct Mater.* **19**, 3632–3637 (2009).
18. Kubo, M. *et al.* Stretchable microfluidic radiofrequency antennas. *Adv Mater.* **22**, 2749–2752 (2010).
19. Yu, Y., Zhang, J. & Liu, J. Biomedical implementation of liquid metal ink as drawable ECG electrode and skin circuit. *PLoS ONE.* **8**, e58771 (2013).
20. Morley, N. B., Burris, J., Cadwallader, L. C. & Nornberg, M. D. GaInSn usage in the research laboratory. *Rev Sci Instrum.* **79**, 056107 (2008).
21. Liu, T. Y., Sen, P. & Kim, C. J. Characterization of nontoxic liquid-metal alloy Galinstan for applications in microdevices. *J Microelectromech S.* **21**, 443–450 (2012).
22. Sheng, L., Zhang, J. & Liu, J. Diverse transformations of liquid metals between different morphologies. *Adv Mater.* **26**, 6036–6042 (2014).
23. Lee, J. & Kim, C. J. Surface-tension-driven microactuation based on continuous electrowetting. *J Microelectromech Syst.* **9**, 171–180 (2000).
24. Beni, G., Hackwood, S. & Jackel, J. L. Continuous electrowetting effect. *Appl Phys Lett.* **40**, 912–914 (1982).

Acknowledgments

This work is partially supported by the NSFC Grant 51376102 and a Specialized Research Fund for the Doctoral Program of Higher Education.

Author contributions

J.L. conceived, designed the work and wrote part of the manuscript. J.Z. performed all the experiments and wrote the manuscript. L.S. performed part of the experiments. All authors discussed the results and commented on the manuscript.

Additional information

Supplementary information accompanies this paper at http://www.nature.com/scientificreports

Competing financial interests: The authors declare no competing financial interests.

How to cite this article: Zhang, J., Sheng, L. & Liu, J. Synthetically chemical-electrical mechanism for controlling large scale reversible deformation of liquid metal objects. *Sci. Rep.* **4**, 7116; DOI:10.1038/srep07116 (2014).